Insights on the formation and dissociation mechanisms of cyclopentane hydrate obtained by using calorimetry and optical microscopy

Raj Kumar Ramamoorthy, Sébastien Teychené, Isaac Rodríguez-Ruiz, Jean-Philippe Torré

Insights on the formation and dissociation mechanisms of cyclopentane hydrate obtained by using calorimetry and optical microscopy

Raj Kumar Ramamoorthy, Sébastien Teychené, Isaac Rodriguez-Ruiz, Jean-Philippe Torré*

Laboratoire de Génie Chimique, Université de Toulouse, CNRS, INPT, UPS, Toulouse, France
** Corresponding authors: jean-philippe.torre@ensiacet.fr*

Abstract:
Identifying the characteristic properties of gas hydrates – including thermo-physical properties – are essential for determining their formation condition and in turn, controlling their yield/growth-rate for/in various applications/environments. Gathering these properties, during in-situ crystallization of gas hydrates, are rather challenging due to the harsh conditions they form and limited by the lack of co-existence of multiple characterization techniques. Owing to these limitations, crystallization process of some SII type gas hydrates and their characteristic properties are ill-defined. Therefore to unveil the complete picture of crystallization process of SII type gas hydrates, in this study, in-situ formation of a model system "cyclopentane hydrate" was monitored using a customized DSC sample holder with a transparent window on top. To this end, in-situ crystallization of cyclopentane hydrate was simultaneously followed by coupling optical microscopy along with scanning calorimetry. Further, we show that the cyclopentane hydrate formed by consuming a part of fresh water appearing after the fusion of ice instead of at a very low temperature ≤ -20 °C.

Keywords: Gas hydrates; calorimetry; optical microscopy; in-situ crystallization; cyclopentane

1. Introduction:

Understanding the crystallization process of gas hydrates is essential for a wide range of areas, including identifying their inhibiting conditions to avoid blockage of gas/oil pipelines (Hammerschmidt, 1934; Heng-Joo and Chin-Jung, 1987), and controlling their yield for secondary refrigeration (Skovborg and Rasmussen, 1994; Galfré et al., 2014; Koh et al., 2011), and gas storage applications (Khurana et al., 2017; Karanjkar et al., 2012). Generally, hydrates are ice-like crystals formed at low temperatures and high

pressures (Koh et al., 2011; Khurana et al., 2017) by combining water (host) and gas (guest) molecules with an appropriate stoichiometric ratio. Owing to these harsh conditions (Karanjkar et al., 2012a) and complex phenomena at water/gas interface (Warrier et al., 2016), capturing such crystallization process, using common lab facilities, is quite challenging. Nevertheless, to unveil such a complex process, a very few in-situ studies of hydrate formation – in suitable sample environments – have been performed using X-ray diffraction (XRD) (Fouconnier et al., 2006), optical microscopy (Sun et al., 2019), Raman spectroscopy (Stern et al., 1998) and differential scanning calorimetry (DSC) (Davies et al., 2010a; Davies et al., 2010b).

In this context, trichlorofluoromethane (CCl_3F) and cyclopentane (CP) hydrates were found to appear after the beginning of ice melting using XRD (Fouconnier et al., 2006) and optical microscopy (Sun et al., 2019; Stern et al., 1998), respectively. In another study, using optical microscopy (Delroisse et al., 2018), CP hydrate was found to emerge above the equilibrium temperature of ice, and their growth rates were found to be in relation with the super-cooling temperature. Taking advantage of these findings, both Raman spectroscopy (Davies et al., 2010a) and DSC studies (Davies et al., 2010b) were performed to determine the mass transfer of guest (methane) and water molecules during the crystallization of methane hydrate. Subsequently, water molecules were found to be highly mobile in the hydrate layer and its growth rate was found to be controlled by the experimental sub-cooling temperatures. In continuation, thermo-physical properties such as equilibrium temperature and enthalpy have been successfully estimated, for various gas hydrates, using DSC (Davies et al., 2010b; Delroisse et al., 2018; Torré et al., 2020; Martinez et al., 2008).

Seemingly, most of the thermo-physical properties of gas hydrates were derived by considering that hydrates are forming during or after the beginning of ice melting. However, this assumption is not precise and may not be sufficient to describe the complete picture of crystallization process, involving different guest molecules, for the following reasons: For the CP/water system, CP hydrate forms immediately after the emergence of water from ice melt whereas CCl_3F hydrate forms at the far end of ice melting. Therefore, overlooking such pivotal information would result in an ill-defined

crystallization process and in turn, in a lack of information on their inhibiting conditions and thus a poor control on the final yield of gas hydrates.

Therefore, to unveil the formation mechanism of gas hydrates, in particular, naturally forming ones, identifying a model system is essential. Among many gas hydrates, CP hydrate, formed by the stoichiometric ratio of 17 H_2O molecules and one CP molecule, is a suitable candidate for understanding the crystallization processes occurring in petroleum pipelines and in sea beds, due to its mild formation condition (below 7 °C and ambient pressure: Nakajima et al., 2008) and a SII crystal structure (each unit cell is composed of 16 small cavities forming pentagonal dodecahedrons and 8 large cavities forming hexadecahedrons: Sloan and Koh, 2008). Thus, monitoring in-situ crystallization of "this model system" using optical microscopy in coupling with either structural or thermal experiments would be an ideal combination to provide new insights on the crystallization process of SII type gas hydrates.

To the best of our knowledge, for the first time, in this study, in-situ crystallization of CP hydrate was simultaneously captured by using optical microscopy in coupling with single-cell scanning calorimetry (SCSC). These complementary and simultaneous observations show that the CP hydrate forms immediately after the beginning of ice melting and its yield is found to be controlled by the heating rate (around ice melting) and the number of experimental cycles.

2. Materials and Methods:

Cyclopentane (purity: ≥ 99.0%), purchased from Sigma-Aldrich, and deionized water were used for all experiments. CP was used without further purification. All experiments were performed in quiescent conditions. In this study, SCSC (DSC Linkam 600: attached with a cryostat device) along with optical microscopy were used to follow the CP hydrate crystallization (please see supplementary information (**Fig. S1**) for the coupled configuration). To couple both SCSC and optical microscopy, first, standard DSC lids were pierced and sealed by transparent polymer: NOA 88. Second, for each experiment, *ca.* 25-28 µl of water and 15 µl of CP were loaded into a DSC pan and hermetically sealed by a customized DSC lid with the transparent NOA 88 window. Either two or three temperature cycles were programmed for each experiment. Typically,

(i) the cooling cycle was performed at the rate of 5 °C/min from room temperature to ~ -22 °C and (ii) the heating cycle was performed by using three different heating rates: from ~ -22 °C to ≈ -2 °C at the rate of 5 °C/min, from -2 °C to 3 °C at the rate between 0.06 and 0.18 °C/min (at the step of 0.06 °C/min) and from 3 °C to the dissociation of CP hydrate at the rate of 1 °C/min. Henceforth, experiments will be named by the heating rate set during the ice melting: CPGH1 (0.06 °C/min), CPGH2 (0.12 °C/min), and CPGH3 (0.18 °C/min). Simultaneously, an optical image of water/CP system was recorded every 0.552 s (exposure time: 0.3 s + time interval: 0.252 s) using a high-speed Imager sCMOS from LAVISION. The enthalpy of fusion of ice and dissociation of hydrate, in standard units (J/mol), were derived with the help of a calibration constant, which was estimated using standard reference samples (alkanes), as described in the reference (Skovborg and Rasmussen, 1994).

3. Results and Discussion:

3.1. In-situ physical changes of CP/water system using optical microscopy in coupling with SCSC:

To unveil the crystallization process of CP hydrate, physical changes of the CP/water system were followed as a function of experimental (cooling and heating) cycles. For simplicity, selected optical images along with the evolution of calorimetric signal of systems (CPGH1 and CPGH2), during their second experimental cycle, are displayed in **Fig. 1 and 2**, respectively. Please refer to high-speed videos (supplementary information: **Video S1** and **Video S2**), for the continuous evolution of systems: CPGH1 and CPGH2, respectively. Irrespective of the experimental conditions, ice formation and melting, and hydrate formation and dissociation are directly visualized and traced using optical microscopy and SCSC, respectively. During the cooling cycle, even after crossing the equilibrium temperature of ice i.e. 0 °C, the CP/water system remains unperturbed. Once the system reaches ca. -18 °C, the beginning of crystallization is directly visualized by the optical recording, and the same is confirmed by the sudden increase of calorimetric signal (the measured exotherm is proportional to the heat released by the crystallization process) using SCSC. This transition completes around -20 °C, which is evidenced by the single exothermic peak. The homogenous contrast of solid phase, along with a few droplets (for CPGH1), confirms that the solid phase is made up of H_2O,

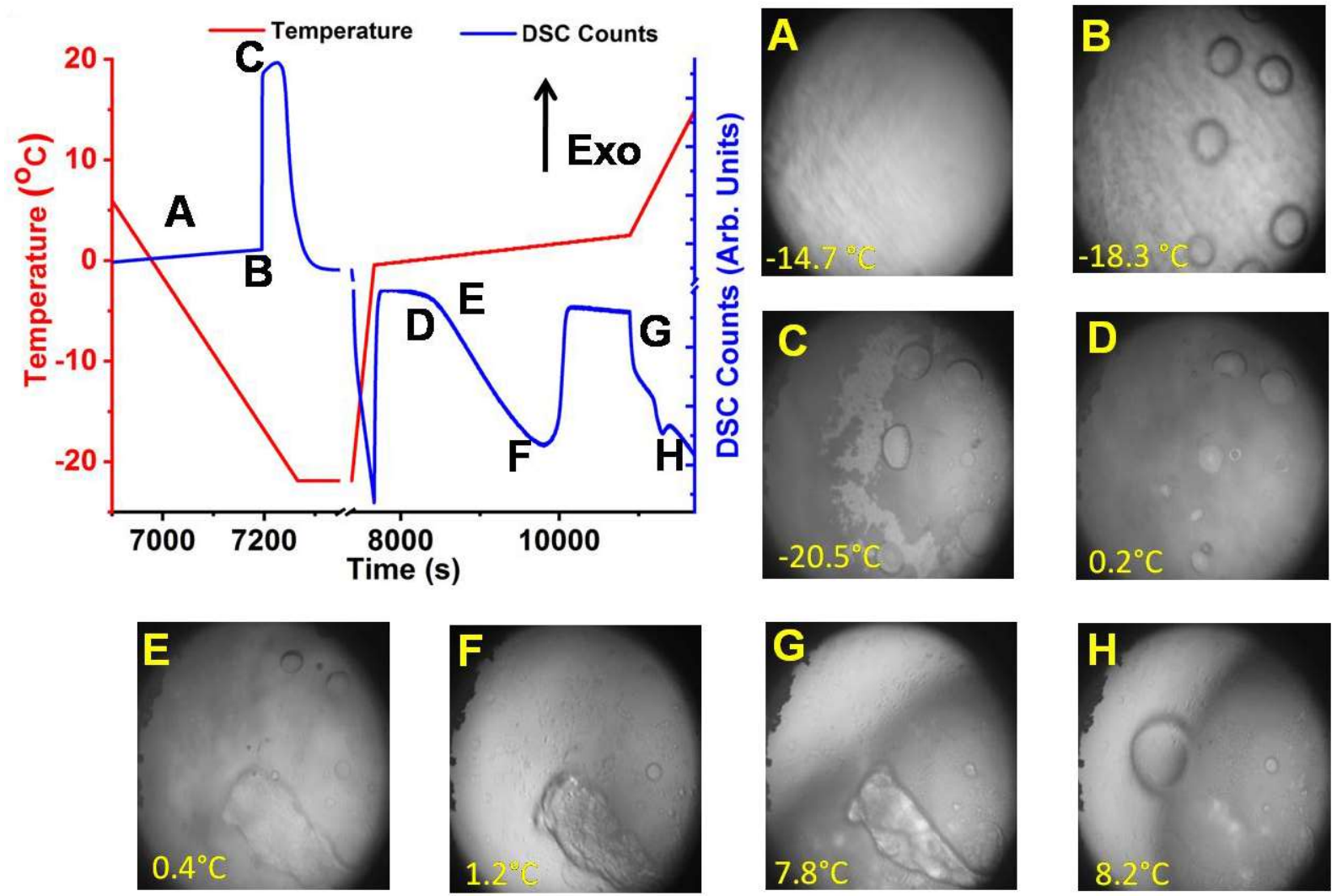

Figure 1. Calorimetric and temperature traces, along with the selected optical images (displayed as a function of increasing time: from A to H), during the second experimental cycle: CPGH1.

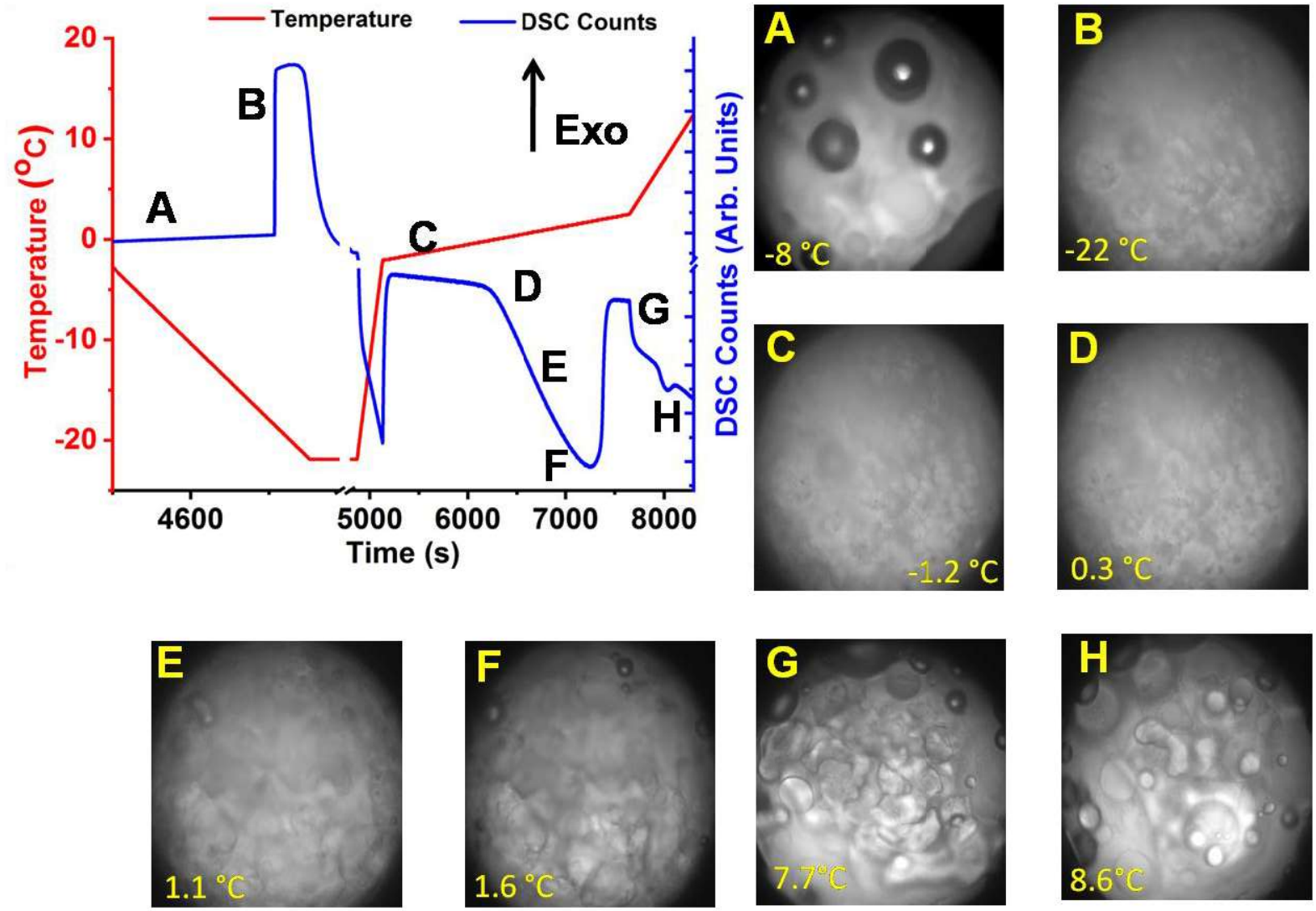

Figure 2. Calorimetric and temperature traces, along with the selected optical images (displayed as a function of increasing time: from A to H), during the second experimental cycle: CPGH2.

as observed by (Sun et al., 2019), instead of both H_2O and H_2O/CP. During the heating cycle, after holding at -22 °C, the physical appearance of solid-phase remains unmodified. Once the system approaches 0 °C, ice melts into liquid water.

With further increase in temperature and time, a new solid-phase emerges all over the recording region by consuming a part of the fresh water coming from ice melt. This process cannot be captured by SCSC due to the dominant endothermic peak of ice fusion. Within the focal plane, we observe that this phase appears close to the equilibrium temperature of ice i.e. very close to the beginning of ice melting but not until the completion of ice melting: between 2 and 3 °C. This observation is consistent with a previous study of CP hydrate (Sun et al., 2019) but in contradiction to the formation of CCl_3F (Fouconnier et al., 2006) and THF (Muro et al., 2012) hydrates, wherein hydrates form at the far end of ice melting and below the equilibrium temperature of ice, respectively. With the further temperature increase, the endothermic peak of ice to water transition completes along with the appearance of a new endothermic peak well-separated from the former (ca. $\Delta T \sim 4$ °C). The corresponding optical observation during the second endothermic peak displays the disappearance of the newly formed phase, along with the appearance of a large number of tiny bubbles. The onset of this dissociation begins ca. 7.0 ± 1.0 °C, which confirms that the newly formed phase during the ice melting is CP hydrate, as previously reported (Fouconnier et al., 2006; Sun et al., 2019).

3.2 Enthalpy of CP hydrate dissociation and water to CP hydrate conversion rate – SCSC:

After determining the relevance of experimental conditions on hydrate formation, a series of experiments were performed to quantify the hydrate formation in relation with the heating rate (close to the temperature of ice fusion), and the number of thermal cycles, using SCSC. The resulted calorimetric and temperature records are plotted as a function of time in **Fig. 3**. The amount of water involved in the hydrate formation was estimated after subtracting the weight of water involved in the first endothermic peak from its initial weight. Then, the water to hydrate conversion rate, as a function of heating rate and experimental cycles, was estimated by following the procedure

described by N. Gaikwad and coworkers (Gaikwad et al., 2021). Their values, as a function of heating rate and experimental cycles, are summarized in the **Table. 1**.

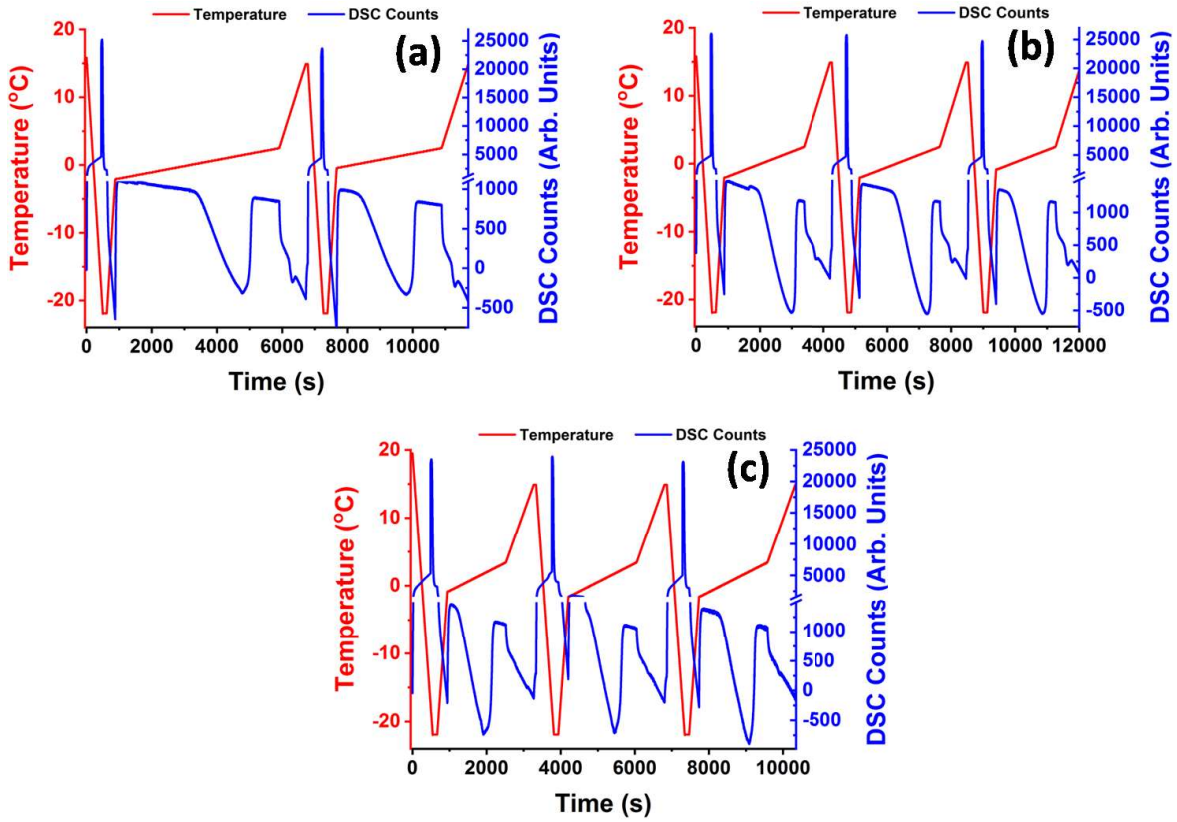

Figure 3. Calorimetric and temperature traces in relation with cooling and heating cycles: (a) CPGH1, (b) CPGH2, and (c) CPGH3.

Table 1: Total weight of CP hydrate and water to hydrate conversion after the completion of each experimental cycle

	Weight of CP hydrate: CPGH1 (mg)	Water to hydrate conversion %	Weight of CP hydrate: CPGH2 (mg)	Water to hydrate conversion %	Weight of CP hydrate: CPGH3 (mg)	Water to hydrate conversion %
First Cycle	0.56	1.65	0.32	0.94	0.02	0.05
Second Cycle	0.58	1.71	0.46	1.36	0.09	0.29
Third Cycle			0.63	1.86	0.11	0.36

Consequently, we found that the yield of hydrate formation increases and decreases with the number of experimental cycles and increasing heating rate, respectively, as observed for CP hydrates in a water-in-oil emulsion (Karanjkar et al., 2012b). This confirms that even with several thermal cycles hydrate formation performed in quiescent condition – resulting in a static interface between water and CP – is not favorable to achieve high water to hydrate conversion rates. Further, irrespective of experimental conditions, the onset, and enthalpy of hydrate dissociation are found to be ca. 7.0 ± 1.0 °C and 115,600 ± 4,500 J/mol, respectively, which is in agreement with the result of Delroisse et al., 2018 but 3% off from Nakajima et al., 2008; and Torré et al., 2020. Therefore, in the future, the crystallization process of CP hydrate in presence of various additives such as surfactants – i.e. sodium dodecyl sulphate – would be followed using optical microscopy in coupling with scanning calorimetry. Such investigations would be very useful to deeply understand how such additives modify the crystal morphology, the formation kinetics, and the water to hydrate conversion.

4. Conclusions:

In-situ formation and dissociation of CP hydrate, as a function of heating rates (close to the equilibrium temperature of ice) and experimental cycles, were followed using optical microscopy in coupling with SCSC. Using these in-situ studies, we demonstrate that CP hydrate forms close to the equilibrium temperature of ice, especially, after the appearance of fresh water from ice fusion instead of either at the far end of ice melting, as observed for CCl_3F or below the equilibrium temperature of ice, as observed for THF hydrate. Further, CP hydrate formation was found to be enhanced with a slow heating rate (close to the equilibrium temperature of ice) and the number of experimental cycles. Nevertheless, even after the third experimental cycle, the inadequate quiescent condition leads to an extremely low conversion rate of CP hydrate from water. We believe that the presented experimental approach would pave a way for more hybrid experiments helping to clarify and describe the crystallization process of hydrates and in turn, provide a lever to control the final yield of gas hydrates for various applications including gas storage and transportation.

Appendix A:

Supplementary data associated with this article can be found in the Supporting Information.

Acknowledgments:

This work was supported by the French Agence Nationale de la Recherche (ANR) [grant number ANR-18-CE05-0028], and undertaken in the frame of the US Partnership for International Research and Education program (National Science Foundation Award Number 1743794) and of the French Research Consortium "GDR-2026 Hydrates de gaz". Further, the authors would like to acknowledge all the people involved in the ANR MUSCOFI project for their valuable scientific input and discussions.

Declaration of Competing Interest:

The authors declare that they have no known competing financial interests or personal relationships that could have appeared to influence the work reported in this paper.

Funding sources :

This work was funded by the French Agence Nationale de la Recherche (ANR) [grant number ANR-18-CE05-0028].

References:

Davies, S. R., Sloan, E. D., Sum, A. K., Koh, C. A., 2010a. In situ studies of the mass transfer mechanism across a methane hydrate film using high-resolution confocal raman spectroscopy. J. Phys. Chem. C, 114, 1173–1180.

Davies, S. R., Lachance, J. W., Sloan, E. D., Koh, C. A., 2010b. High-pressure differential scanning calorimetry measurements of the mass transfer resistance across a methane hydrate film as a function of time and subcooling. Ind. Eng. Chem. Res., 49, 12319–12326.

Delroisse, H., Plantier, F., Marlin, L., Dicharry, C., Frouté, L., André, R., Torré, J-P., 2018. Determination of thermophysical properties of cyclopentane hydrate using a stirred calorimetric cell. J. Chem. Thermodyn., 125, 136–1412.

Fouconnier, B, Komunjer, L., Ollivon, M., Lesieur, P., Keller, G., Clausse, D., 2006. Study of CCl_3F hydrate formation and dissociation in W/O emulsion by differential scanning calorimetry and X-ray diffraction. Fluid Ph. Equilibria, 250, 76–82.

Gaikwad, N., Nakka, R., Khavala, V., Bhadani, A., Mamane, H., Kumar, R., 2021. Gas hydrate-based process for desalination of heavy metal ions from an aqueous solution: Kinetics and rate of recovery. ACS ES&T Water, 1, 134–144.

Galfré, A., Kwaterski, M., Braîntuas, P., Cameirao, A., Herri, J. M., 2014. Clathrate hydrate equilibrium data for the gas mixture of carbon dioxide and nitrogen in the presence of an emulsion of cyclopentane in water. J. Chem. Eng. Data., 59, 592–602.

Hammerschmidt, E. G., 1934. Formation of gas hydrates in natural gas transmission lines. Ind. Eng. Chem., 26, 851–855.

Heng-Joo, N. G, Chin-Jung, G., 1987. Hydrate formation and inhibition in gas condensate and hydrocarbon liquid systems. Fluid Ph. Equilibria, 36, 99-106.

Ho-Van, S., Bouillot, B., Garcia, D., Douzet, J., Cameirao, A., Maghsoodloo-Babakhani, S., Herri, J-M., 2019. Crystallization mechanisms and rates of cyclopentane hydrates formation in brine. Chem. Eng. Technol., 42 (7), 1481–1491.

Karanjkar, P. U., Lee, J. W., Morris, J. F., 2012a. Surfactant effects on hydrate crystallization at the water−oil interface: Hollow-conical crystals. Cryst. Growth Des., 12, 3817−3824.

Karanjkar, P. U., Lee, J. W., Morris, J. F., 2012b. Calorimetric investigation of cyclopentane hydrate formation in an emulsion. Chem. Eng. Sci., 68, 481–491.

Khurana, M., Yin, Z., Linga, P., 2017. A review of clathrate hydrate nucleation. ACS Sustainable Chem. Eng., 5, 11176−11203.

Koh, C.A., Sloan, E.D., Sum, A. K.., Wu, D. T., 2011. Fundamentals and applications of gas hydrates. Annu. Rev. Chem. Biomol. Eng., 2, 237–57.

Martinez, M. C., Dalmazzone, D., Furst, W., Delahaye, A., Furnaison, L., 2008. Thermodynamic Properties of THF + CO_2 hydrates in relation with refrigeration applications. AIChE J., 54(4), 1088-1095.

Muro, M., Harada, M., Hasegawa, T., Okada, T., 2012. Formation and growth of tetrahydrofuran hydrate at the ice/hexane interface. J. Phys. Chem. C, 116, 13296−13301.

Nakajima, M., Ohmura, R., Mori, Y. H., 2008. Clathrate hydrate formation form cyclopentane-in-water emulsion. Ind. Eng. Chem. Res., 47, 8933–8939.

Sloan, E. D., Koh, C. A., 2008. Clathrate hydrates of natural gases. 3rd edition., CRC press, New York

Skovborg, P., Rasmussen, P., 1994. A mass transport limited model for the growth of methane and ethane gas hydrates. Chem. Eng. Sci., 49, 1131–1143.

Stern, L. A., Hogenboom, D. L., Durham, W. B., Kirby, S. H., Chou, I-M., 1998. Optical-cell evidence for superheated ice under gas-hydrate-forming conditions. J. Phys. Chem. B, 102, 2627-2632.

Sun, Q., Du, M., Li, X., Guo, X., Yang, L., 2019. Morphology investigation on cyclopentane hydrate formation/dissociation in a sub-millimeter-sized capillary. Crystals, 9, 307.

Torré, J-P., Plantier, F., Marlin, L., André, R., Haillot, D., 2020. A novel stirred micro calorimetric cell for DSC measurements applied to the study of ice slurries and clathrate hydrates. Chem. Eng. Res. Des., 160, 465–475.

Warrier, P., Khan, M. N., Srivastava, V., Maupin, C. M., Koh, C. A., 2016. Overview: Nucleation of clathrate hydrates. J. Chem. Phys., 145, 211705.